



VCU

Virginia Commonwealth University
VCU Scholars Compass

Theses and Dissertations

Graduate School

2013

The Effects of Tarsh Overexpression on Lung Carcinomas

Young Kim
Virginia Commonwealth University

Follow this and additional works at: <https://scholarscompass.vcu.edu/etd>



Part of the [Physiology Commons](#)

© The Author

Downloaded from

<https://scholarscompass.vcu.edu/etd/498>

This Thesis is brought to you for free and open access by the Graduate School at VCU Scholars Compass. It has been accepted for inclusion in Theses and Dissertations by an authorized administrator of VCU Scholars Compass. For more information, please contact libcompass@vcu.edu.

School of Medicine
Virginia Commonwealth University

This is to certify that the thesis prepared by Young Min Kim entitled THE EFFECTS OF TARSH OVEREXPESSION ON LUNG CELL CARCINOMAS has been approved by his or her committee as satisfactory completion of the thesis requirement for the degree of Master of Science in Physiology.

Dr. Hiroshi Miyazaki, M.D., Ph.D., Phillips Institute, VCU School of Dentistry

Dr. Hisashi Harada, Ph.D., Massey Cancer Center, VCU School of Dentistry

Dr. Christina Marmarou, Ph.D., Department of Neurosurgery, VCU School of Medicine

Dr. Roland Pittman, Ph.D., Department of Physiology and Biophysics, VCU School of Medicine

Dr. Leon Avery, Ph.D., Chair of the Graduate Department of Physiology and Biophysics, VCU School of Medicine

Dr. Jerome, F. Strauss III, M.D., Ph.D, Dean of the VCU School of Medicine

Dr. F. Douglas Boudinot, Dean of the Graduate School

April 26, 2013

© Young Min Kim, 2013

All Rights Reserved

THE EFFECTS OF TARSH OVEREXPRESSION ON LUNG CELL CARCINOMAS

A Thesis submitted in partial fulfillment of the requirements for the degree of Master of Science at Virginia Commonwealth University.

by

YOUNG MIN KIM

Post-baccalaureate Certificate, Virginia Commonwealth University, 2011
Biological Sciences, BS, 2007

Director: DR. HIROSHI MIYAZAKI

ASSISTANT PROFESSOR OF ORAL AND CRANIOFACIAL MOLECULAR
BIOLOGY

Virginia Commonwealth University
Richmond, Virginia
May 2013

Acknowledgements

Above all, I would like to thank my primary investigator and advisor, *Dr. Hiroshi Miyazaki*, for his willingness to undertake the task of mentoring me as a student in his lab. I will always thank him for his guidance and encouragement throughout my Masters study this year. With the help of his knowledge and experience in lung cancer biology, I was able to understand the complex molecular mechanisms involved in my field of research. His unwavering patience and oversight over my experiments has contributed to my success as a student and researcher. In addition, I would like to thank my co-advisor, *Dr. Hisashi Harada*, for his expertise with PCR and for permitting me to perform experiments in his lab at Massey Cancer Center. I also thank *Dr. Andrew Yeudall* for his recommendations on how to improve my project. I am grateful to *Dr. Christina Marmarou* and *Dr. Roland Pittman* for becoming a part of my committee, as well as for their input and support. *Mark Hicks* must be acknowledged for assisting me with PCR experiments and for making my time at Massey Cancer Center enjoyable. Finally, I would like to acknowledge my colleague and lab partner, *Rubana Masood*, for her constant support.

Table of Contents

	Page
Acknowledgements	iv
List of Tables	viii
List of Figures	ix
Abstract	xi
Chapter	
1 Introduction	1
1.1: Cancer	1
1.2: Lung Cancer Cell Carcinoma	5
1.3: p53 and its Effects on Cancer	6
1.4: Tarsh and Cellular Senescence	8
1.5: Interactions Between p53 and Tarsh	10
1.6: Implications of Tarsh in Lung Cancer	11
1.7: Hypothesis and Rationalization for the Current Study	12
2 Materials and Methods	13
2.1: Cell Lines and Culture	13
2.1.1: Cell Line Preparation	13
2.1.2: Tarsh Transfection and Knockdown of p53	14
2.1.3: Cell Maintenance	14
2.1.4: Cell Stock Preparation	15
2.2: Reagents and Antibodies	15
2.3: RNA Extraction	16

2.4: Reverse Transcription.....	16
2.5: Quantitative Real-Time Polymerase Chain Reaction.....	17
2.6: Western Blot.....	18
2.7: Cell Proliferation Assay	19
2.8: Cell Migration Assay.....	20
2.9: Statistical Analysis	21
3 Results	22
3.1: Tarsh Expression Confirmation with qRT-PCR Analysis	22
3.2: p53 Downregulation Confirmation with qRT-PCR Analysis	24
3.3: p53 Protein Expression Confirmation with Western Blot.....	26
3.4: Tarsh Overexpression Suppresses Proliferation in All Cell Lines	28
3.5: p53 Downregulation Increases Proliferation in All Cell Lines	32
3.6: Tarsh Suppresses A549 Migration, H1299 Migration Unaffected.....	33
3.7: Role of p53 in Migration is Unclear.....	37
4 Discussion	38
4.1: Aims of the Current Study.....	38
4.2: Lung Cancer Cell Carcinoma (LCCC) Model System.....	38
4.3: Role of p53 and Tarsh in Cell Proliferation	40
4.4: Role of p53 and Tarsh in Cell Migration	41
4.5: Conclusions	43
4.6: Future Studies.....	43
References.....	45
Vita.....	51

List of Tables

	Page
Table 1: Lung Cancer Stage Distribution and 5-year Survival.	6

List of Figures

	Page
Figure 1: Cancer Rates Attributable to Smoking	4
Figure 2: Lung Cancer Stage Distribution and 5-year Survival.....	7
Figure 3: Tarsh Expression in 15 Lung Cancer Strains	9
Figure 4: Tarsh Expression in p53 KD MEFs.....	11
Figure 5: Hemocytometer Counting.....	20
Figure 6: Tarsh Expression	23
Figure 7: p53 Gene Expression	25
Figure 8: Western Blot Analyzing p53 Protein Expression.....	27
Figure 9: A549 WT Proliferation.....	29
Figure 10: A549 p53 KD Proliferation	30
Figure 11: H1299 Proliferation	31
Figure 12: Cell Migration Assay.....	34
Figure 13: Role of Tarsh in A549 Migration	35
Figure 14: H1299 Migration	36

List of Abbreviations

BSA	Bovine Serum Albumin
CKI	Cyclin-Dependent Kinase Inhibitor
CNS	Central Nervous System
KD	Knockdown
LCCC	Lung Cancer Cell Carcinoma
MEFs	Mouse Embryonic Fibroblasts
p53	Protein 53
PBS	Phosphate-Buffered Saline
ROS	Reactive Oxygen Species
Δ RQ	Relative Quantification
SA- β -gal	Senescence-Associated β -Galactosidase
shRNA	Short Hairpin RNA
TBST	Tween-20
qRT-PCR	Quantitative Real-Time Polymerase Chain Reaction
UV	Ultraviolet
WT	Wild-Type

Abstract

THE EFFECTS OF TARSH OVEREXPRESSION ON LUNG CELL CARCINOMAS

By Young Min Kim, M.S.

A Thesis submitted in partial fulfillment of the requirements for the degree of Master of Science at Virginia Commonwealth University.

Virginia Commonwealth University, 2013.

Major Director: Dr. Hiroshi Miyazaki, M.D., Ph.D.
Philips Institute, VCU School of Dentistry

Lung cancer arises from epithelial cells that line the air passages of the lungs. It is the second most common malignancy in the United States; trends suggest that over 228,000 new patients will be diagnosed with lung cancer in 2013. Due to the fact that lung cancer is highly aggressive, it has proven difficult to control. The 5-year survival rate has been shown to be only 15.9%, despite the advances made in terms of diagnosis and treatment. Therefore, we are faced with the problem of finding more effective methods that allow for an earlier diagnosis and the improved treatment of lung cancer. This study attempts to address these issues by investigating Tarsh, a novel molecule that is involved in the regulation of cellular senescence. Previous studies have shown that Tarsh is expressed in normal lung cells, but is significantly downregulated in lung tumors. These studies also

determined that Tarsh is likely dependent upon the expression of p53, a tumor suppressor gene. The current study investigated these results, in addition to the biological effects of ectopically increasing Tarsh and/or knocking down p53 expression in two lung cancer cell lines: A549 and H1299 cell lines. It was determined that increasing the expression of Tarsh decreased the rate of proliferation in both cell lines. Additionally, it was shown that the knockdown of p53 increased proliferation in A549 cells. In regards to the migration rate of these cell lines, the overexpression of Tarsh decreased migration in A549 cells, but had no effect on H1299 cells. However, the role of p53 in migration is still unclear. The results of this study suggest that the knockdown of p53 decreases cell migration in A549 cells. This contradicts the fact that H1299 cells do not express p53, yet was found to have the highest migration rate. It is evident that a further investigation is needed to make more concrete conclusions. Nevertheless, the suppressive features of Tarsh on cell proliferation, and possibly migration, make it a promising target of research for lung cancer therapy.

Introduction

1.1: Cancer

Each year, cancer causes about 570,000 deaths, equating to about 25% of the annual mortalities, in the United States⁽⁷⁾. In addition, cancer affects people on a global scale, claiming numerous lives due to its high adaptability. In essence, it is an ailment involving the uncontrolled growth of cells in the body. Failure rates with treatment, and high mortality rates associated with cancer, can be contributed to the ability of these cells to metastasize. This results in the spreading of the cells to adjacent tissues, and eventually distant organs⁽³⁾.

Cancer types may be grouped into five categories, which include carcinomas, sarcomas, leukemias, lymphomas, and cancers of the central nervous system (CNS). Carcinomas are cancers that arise from the skin, or in tissues that border internal organs. Carcinomas can be further divided into subtypes, based on their histology. These subdivisions include adenocarcinomas, basal cell carcinomas, squamous cell carcinomas, and transitional cell carcinomas. Sarcomas are cancers that originate in connective or supportive tissue, such as cartilage, bone, muscle, fat, and blood vessels. Leukemias develop from blood-forming tissues, and produce an excess of abnormal white blood cells. These abnormal cells eventually replace pre-existing, normal white blood cells.

Lymphomas are cancers that involve the lymphatic system, a subdivision of the immune system. These cancers may be categorized as either Hodgkin type lymphomas, which develop from abnormal B-cells, or non-Hodgkin type lymphomas, which develop from abnormal B-cells or T-cells. Finally, CNS cancers start in the tissues of the brain and spinal cord, and arise mainly from astrocytes, the cerebellum, or the spinal cord⁽¹⁸⁾.

Regardless of origin, however, all cancers are believed to be the product of genetic mutations in normal cells. These newly transformed cells result in a tumor phenotype, and they often gain the ability to proliferate, survive, and invade surrounding tissues without limit. Under normal circumstances, these physiological processes are highly regulated. However, in the case of tumor phenotypes, the deregulation of these processes leads to cancer metastasis. The downregulation of these inhibitory effects may be linked to mutations in tumor-suppressor genes. Normally, these genes function to limit cell growth, but their inactivation during cancer leads to uncontrolled proliferation. The activation of another set of genes, known as proto-oncogenes, may also result in a cancer phenotype. These genes function to enhance cell growth, and in cancer, their levels are overexpressed. It is likely that mutations in both tumor-suppressor and proto-oncogenes act synergistically. Therefore, a combination of mutations in both of these genes may cause abnormal protein expression and characteristics that lead to tumor phenotypes⁽¹¹⁾.

Environmental factors that contribute to the genetic mutations associated with cancer include smoking, alcohol, and ultraviolet (UV) radiation exposure. Routinely consuming alcohol significantly increases the risk of developing cancer. Previous studies have shown a positive correlation between alcohol consumption and cancer development,

particularly in upper aerodigestive tract carcinomas. Specifically, ethanol has been found to be the main culprit responsible for cancer formation. Ethanol can aid in the absorption of other carcinogens by acting as a solvent for entrance into the mucosal tissues. As a result, using alcohol with other drugs can have synergistic effects. Previous studies suggest that the effects of alcohol and smoking are multiplicative. About 75% of aerodigestive tract carcinomas can be credited to the simultaneous use of alcohol and tobacco. In addition, various *in vivo* and *in vitro* studies suggest that the metabolic byproduct of alcohol, acetaldehyde, possesses toxic effects. Acetaldehyde has the ability to disrupt DNA synthesis, DNA repair sites, and the checkpoints involved in cell replication. Therefore, ethanol and acetaldehyde synergistically promote cancer development^(20,29).

The chemicals in tobacco smoke are also associated with cancer, producing damaging effects on DNA. Benzo(a)pyrene, which binds to cells in the airways and organs of smokers, has been shown to be the most damaging carcinogen in tobacco smoke. Consequently, lung cancer is frequently attributed to smoking. The risk of developing lung cancer is directly associated with the number of cigarettes smoked. Other carcinomas, such as cancers of the bladder, kidney, cervix, oral cavity, stomach, pancreas and esophagus, are also linked to tobacco use⁽¹⁹⁾.

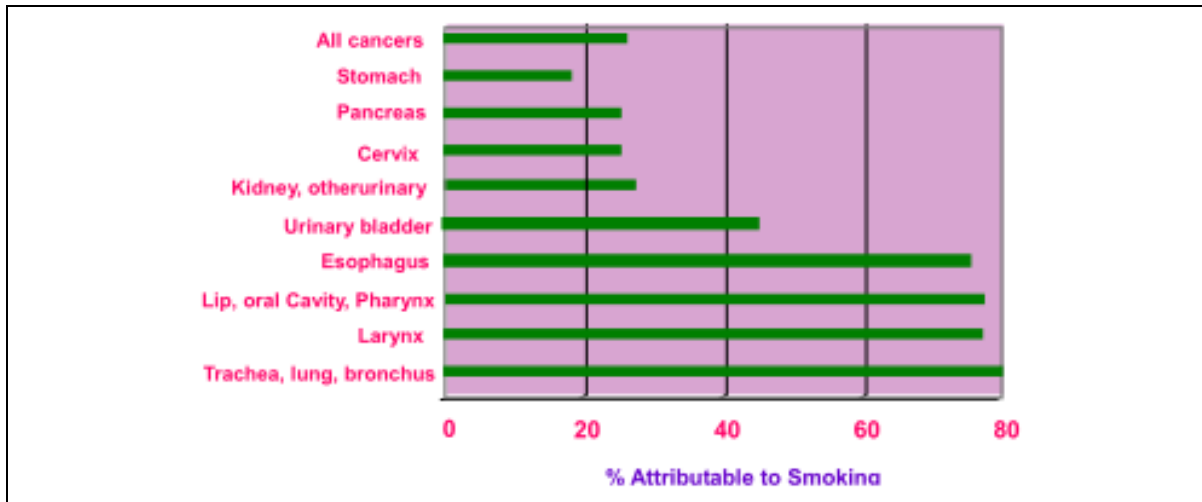


Figure 1: Cancer Rates Attributable to Smoking. The percentage of various cancers caused by smoking. The upper aerodigestive tract is most affected⁽¹⁹⁾.

Ultraviolet (UV) radiation from the sun can lead to the development of various skin cancers, such as cutaneous malignant melanoma, basal cell carcinoma, and squamous cell carcinoma. UV radiation can be divided into three categories (UV-A, UV-B, and UV-C). UV-A and UV-B are usually linked with the development of skin carcinomas in humans. UV-B has the ability to cause direct damage to DNA through the formation of pyrimidine dimers. Whenever DNA repair mechanisms fail, the resulting mutations can propagate to future cell generations via cell divisions. UV-B can also form highly reactive oxygen species (ROS) and damage DNA. Furthermore, UV-A and UV-B radiation can promote the expression of anti-apoptotic proteins. Although preventable, the frequency of skin cancer and mortality has been increasing over the last 10 years^(3,30).

1.2: Lung Cancer Cell Carcinoma

Lung Cancer Cell Carcinoma (LCCC) is the second most common malignancy in the United States; it is estimated that over 228,000 new cases will arise this year. The majority of lung cancers originate from epithelial cells that line the air passages in the lungs. The two most common types of lung cancer are classified based on their histological appearance: small cell lung cancer (SCLC) and non-small cell lung cancer (NSCLC). SCLC accounts for about 12.5% of lung cancer cases. These cells tend to grow aggressively and metastasize quickly. In contrast, NSCLC is responsible for about 87.5% of lung cancer cases. Compared to SCLC, these cells are larger in size and develop more slowly⁽¹⁸⁾. Additionally, studies have shown that the long-term use of tobacco products accounts for 90% of lung cancers⁽⁵⁾. However, it is possible for non-smokers to develop lung cancer as well. Non-smokers may tumors develop due to genetic factors, secondhand smoke, air pollution, radon gas, and asbestos^(5,24).

LCCC treatments are tailored based on the stage and type of lung cancer. In the early stages, the cancer is localized to one side of the chest. If the cancer is aggressive or advanced, it commonly spreads to the lymph nodes and other organs. Lung cancer patients with an early diagnosis may be eligible for surgical removal of the primary tumor. In addition, radiotherapy and chemotherapy are other options available at any stage of the disease⁽¹⁸⁾. Admittedly, lung cancer is difficult to control with current treatments. In addition, only 15% of patients are diagnosed at an early stage. As a result, the 5-year prognosis remains poor. Previous research shows that the overall 5-year survival rate for

2002-2008 was 15.9%⁽⁹⁾. Therefore, it is evident that new, viable treatments are necessary to improve patient survival.

Stage at Diagnosis	Stage Distribution (%)	5-year Relative Survival (%)
Localized (confined to primary site)	15	52.2
Regional (spread to regional lymphnodes)	22	25.1
Distant (cancer has metastasized)	56	3.7
Unknown (unstaged)	6	7.9

Table 1: Lung Cancer Stage Distribution and 5-year Survival. The average 5-year survival rate of cancer patients is compared to that of the general population. The majority of patients are diagnosed when the cancer has advanced to later stages⁽⁹⁾.

1.3: p53 and its Effects on Cancer

Protein 53 (p53) is a well-known tumor suppressor that regulates the cell cycle and apoptosis in multicellular organisms. In humans, it is encoded by the TP53 gene located on chromosome 17^(16,10). Due to its role in maintaining genomic stability, p53 has been described as "the guardian of the genome"⁽²¹⁾. The p53 protein is made of 393 amino acids, and has four domains: a domain that activates transcription⁽²⁶⁾, a core domain that binds DNA⁽¹²⁾, a domain involved in the tetramerization of p53⁽⁶⁾, and a domain that recognizes damaged DNA⁽⁴⁾.

In normal cells, the expression p53 protein is low. However, cellular stresses, such as DNA damage, may increase its production. A rise in p53 expression leads to growth arrest at the G₁/S regulation point in the affected cells, which in turn prevents the replication of damaged DNA. During cell cycle arrest, p53 also activates genes that

produce DNA repair proteins. Once the DNA is repaired, cell cycle inhibition comes to an end. However, if the DNA is irreparable, p53 can initiate apoptosis in the damaged cells. In this manner, the proliferation of cells with abnormal DNA is prohibited⁽²⁾.

Due to the fact that p53 causes potent downstream effects, its expression needs to be regulated. Although it can inhibit tumor growth, high levels of p53 may cause unnecessary apoptosis and result in premature aging. A regulatory gene, Mdm2, functions to regulate the expression of p53. As p53 becomes activated, the expression of Mdm2 is also increased. Mdm2 then downregulates the expression of p53 by labeling it for degradation with ubiquitin⁽²⁾.

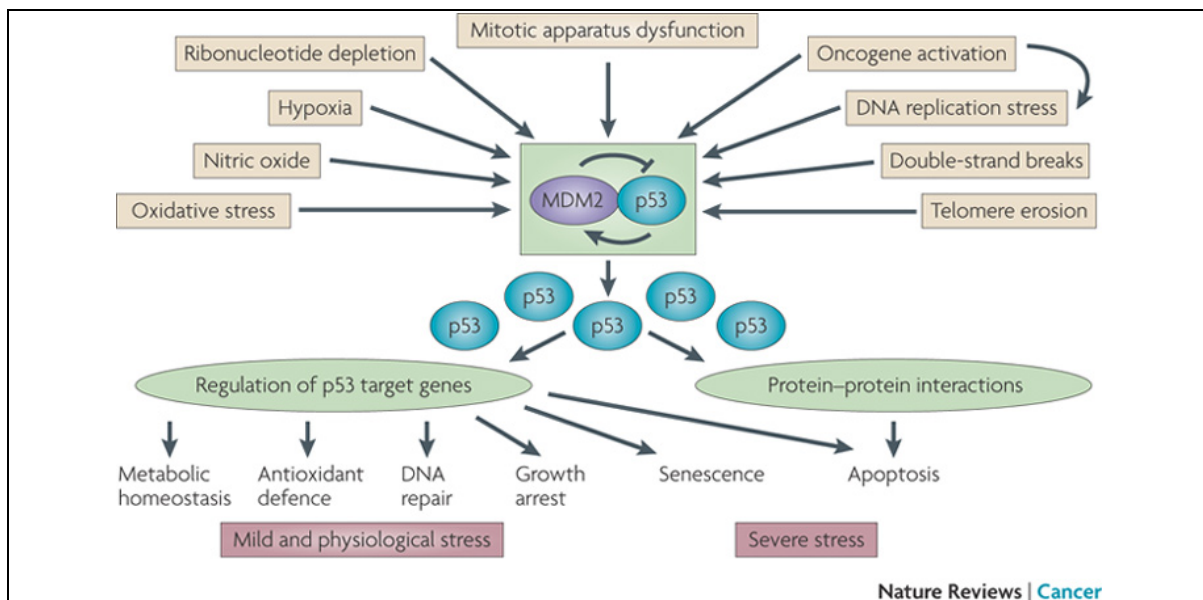


Figure 2: Simplified Scheme of the p53 Pathway. Cellular stress leads to increased expression of p53, which in turn activates downstream genes involved in growth arrest, DNA repair, and apoptosis. Increased p53 expression leads to increased Mdm2 expression, which in turn negatively regulates p53⁽¹⁴⁾.

Defective p53 can result in the reduction of tumor suppression and lead to tumor formation. In over 50% of all cancers, the p53 gene is either mutated or deleted, resulting in the expression of a non-functional mutant p53 protein. This loss-of-function mutation results in the deregulation of the cell cycle and apoptosis, which may lead to the uncontrolled growth of cells. Previous research also implies that p53 plays a role in cell migration and invasion. In addition, recent studies suggest that gain-of-function mutations may occur in p53, which may play a role in promoting cell migration, invasion, and metastasis⁽¹⁷⁾.

The numerous studies on p53 have led to the increased understanding of processes involved in tumorigenesis. Although cancer therapies have yet to be derived from these findings, it is clear that p53 is a powerful mediator of various cell functions, and that the formation of most tumors is dependent on the inactivation of p53. In effect, this makes p53 a valuable target for cancer treatment.

1.4: Tarsh and Cellular Senescence in Lung Cancer

Cellular senescence, or aging, is an unavoidable process that all cells in the body eventually undergo. It was predominantly observed in cultured human fibroblast cells that entered an irreversible non-dividing state. Recent studies have reported that the shortening of telomeres may contribute to this process. Furthermore, these studies have also shown that senescence could be stimulated by extrinsic factors unrelated to telomere length. These factors included oxidative stress, UV exposure, and oncogenic gene activation. The role of other senescence-related genes, such as p53, has been investigated, though not

much is known about the overall process of senescence at this point. However, these studies suggest that senescence is likely involved in the elimination of damaged cells, which in turn suppresses tumor formation⁽²⁵⁾.

Recent findings suggest that Tarsh, a novel target of NESH-SH3, is a molecule involved in the regulation of senescence. Lung carcinomas were specifically chosen because the presence of Tarsh was detected in mouse lung. It was also determined that Tarsh expression increased during senescence of mouse embryonic fibroblasts (MEFs)⁽²⁵⁾. Other results have indicated that Tarsh is strongly expressed in normal lung cells, and that Tarsh is significantly downregulated in lung tumors. This downregulation in expression coincided with a decrease in a tumor's ability to proliferate and invade surrounding areas. These results suggest that the loss of Tarsh in lung cancer cells may contribute to tumorigenesis⁽²³⁾.

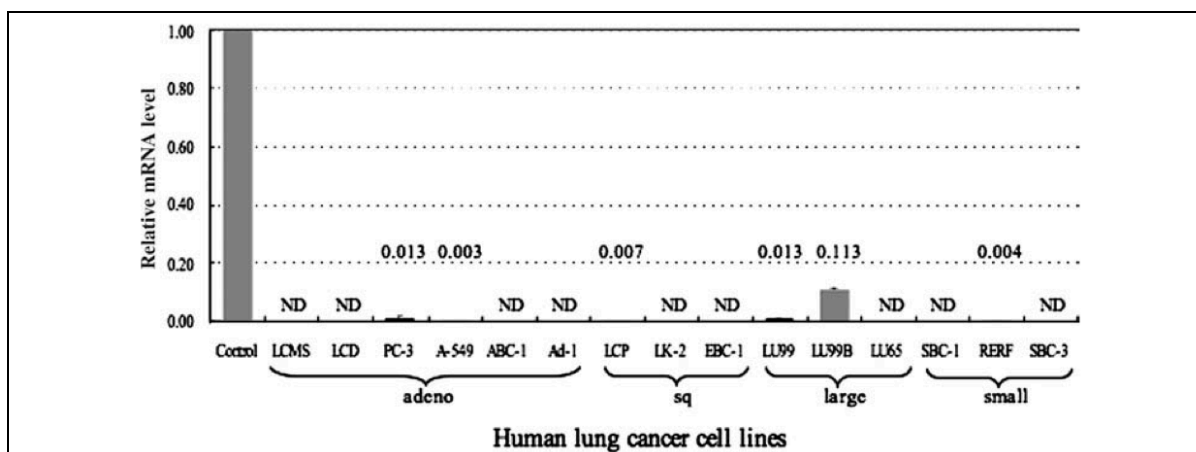


Figure 3: Tarsh Expression in 15 Lung Cancer Strains. The relative mRNA expression of Tarsh in various lung cancer cell lines, compared to that of normal lung cells. A significant reduction in Tarsh expression was observed in all 15 strains⁽²³⁾.

1.5: Interactions Between p53 and Tarsh

Another study investigated a possible link between Tarsh and p53 by using a senescence-associated β -galactosidase (SA- β -gal) activity assay in MEFs. Stained cells would indicate that the cells were aging. In preparation for this assay, the expression of Tarsh was knocked down in previously derived wild type (WT) and p53 knockdown (KD) MEFs. These cells were then compared to WT and p53 KD MEFs with normal Tarsh expression. The results of this study indicated that TARSH suppression lead to a decrease in the staining of MEFs, and therefore reduced cellular senescence⁽²⁸⁾.

The same study also examined the effects of Tarsh suppression on various cancer related genes. Other than p53, only one other gene was activated in response to the downregulation of Tarsh. It was determined that p21, a known p53-dependent cyclin-dependent kinase inhibitor (CKI), was increased in Tarsh-depleted cells⁽²⁸⁾. Generally, p21 suppresses cell growth via the induction of cell cycle arrest and the inhibition of gene transcription and apoptosis. These anti-proliferative properties are important in promoting cellular senescence⁽¹⁾. However, an increase in p21 activity was only observed in WT MEFs, which expressed p53. No increase in p21 was detected in p53 KD MEFs⁽²⁸⁾. These results imply that Tarsh plays a role in p53-dependent cellular senescence in MEFs.

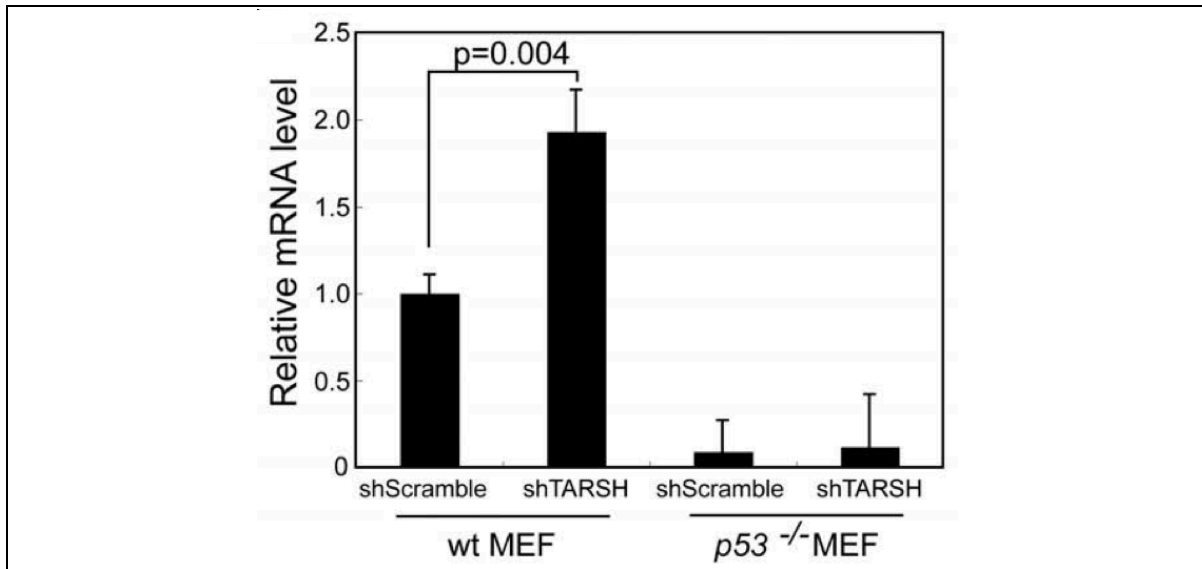


Figure 4: Tarsh Expression in p53 KD MEFs. The relative mRNA expression of Tarsh in p53 KD MEFs, compared to that of WT MEFs. A significant reduction in Tarsh expression was observed in p53 KD MEFs^(kunihiiko).

1.6: Implications of Tarsh in Lung Cancer

As previously discussed, lung cancer is one of the leading causes of mortality in the United States. The 5-year survival rate for lung cancer patients is very low, which can be attributed to the fact that its diagnosis usually occurs in later stages. Therefore, there is a dire need to develop effective methods for the early diagnosis and treatment of lung cancer. Recent studies have demonstrated a significant reduction in the expression of Tarsh in lung tumors. This information may prove to be beneficial in clinical applications; measurements of Tarsh expression in patients could be utilized to determine if cells have become malignant. In addition, further investigation into the mechanisms of how Tarsh contributes to cellular senescence could lead to the development of novel therapies.

1.7: Hypothesis and Rationalization for the Current Study

The rationalization for this study is to further investigate the biological roles of Tarsh and p53 in various lung cancer cell lines. These cell lines include A549 Wild-Type (WT) cells, A549 p53 KD (Knockdown) cells, and H1299 cells. This study will examine *in vitro* proliferation and migration rates of these cells, which express varying levels of p53, depending on the cell line. In turn, the study will verify the effectiveness of Tarsh in regards to tumor suppression, while determining its dependency on p53. The hypothesis of this study is that the overexpression of Tarsh will reduce cancer-development related processes, such as cell proliferation, motility, and survival. In addition, based on previous findings, it is hypothesized that Tarsh is dependent on the presence of p53, and that the effects of Tarsh and p53 may be synergistic.

Materials and Methods

2.1: Cell Lines and Culture

2.1.1: Cell Line Preparation

A549 adenocarcinomic human alveolar basal epithelial cells were originally obtained from a 58-year-old Caucasian male patient (explanted tumor), and H1299 human non-small cell lung carcinoma cells were extracted from a 43-year-old Caucasian male patient (lymph node). The cells were purchased from commercial vendors, and were frozen at -80°C. When ready for use, the cells were placed in a 37°C water bath to thaw. The cells were then suspended in a solution of 10 mL of Dulbecco's modified Eagle's medium (DMEM) (Mediatech, Manassas, VA), 10% Fetal Bovine Serum (FBS), and specific antibiotics depending on the cell line. The A549 WT and H1299 cell medium was treated with 100 µg/mL streptomycin, 100 µg/mL neomycin, and 100 µg/mL puromycin. The A549 p53 KD cell medium was treated with 100 µg/mL streptomycin and 100 µg/mL puromycin. Afterward, the cells were placed on 10 cm tissue culture plates. Each tissue culture plate was placed in a humidified incubator at 37°C with a 10% CO₂ control and 90% air to allow for growth. The cells were washed with phosphate-buffered saline (PBS),

and cultured in the same media solution every two to three days for maintenance until needed.

2.1.2: Transfection of Tarsh and Knockdown of p53

To establish cell lines overexpressing Tarsh, 10 µg of DNA construct was transfected into 5×10^6 A549 WT, A549 p53 KD, and H1299 cells by electroporation using a Gene Pulser II (Bio-Rad Laboratories Inc.). To create controls for each cell type, a pcDNA3.1 vector was transfected into these cells. The resulting clones were isolated after three weeks of selection in neomycin and puromycin selection media. These cells were then seeded onto 10 cm plates and incubated to allow for cell expansion. For each cell line, the expression of Tarsh was determined with quantitative real-time polymerase chain reaction analysis (qRT-PCR).

p53 knockdown in A549 WT and A549 WT Tarsh transfected cells were generated by using lentivirus expressing short hairpin RNA (shRNA) against p53. Lentivirus systems (Open Biosystems) were utilized, following the manufacturer's protocol. Clones were isolated after three weeks of selection in neomycin and puromycin selection medium. These cells were then seeded onto 10 cm plates and incubated to allow for cell expansion. For each cell line, the expression of p53 was determined with qRT-PCR.

2.1.3: Cell Maintenance

Once the cells reached 100% confluency, they were split. The each cell plate was washed twice with 10 mL PBS, and then 1 mL of 0.5% trypsin was added. The cells were

then incubated for 5-15 minutes for detachment. To ensure proper detachment from the plate, the detachment of cells after administration of trypsin were confirmed with the microscope. Afterward, the cells were incubated to allow for continued healthy expansion.

2.1.4: Cell Stock Preparation

Long-term storage of cell lines was prepared by making cell stock solutions in cryovials. 5 mL of media was added via jet flow to each 10 cm plate of cells after detachment with 1 mL of 0.5% trypsin. The cell-media solution was then collected, pipetted into a 15 mL vial, and centrifuged at 800 rpm for 5 minutes at 4 degrees Celsius. After centrifugation, the media supernatant was removed by aspiration, leaving a cell pellet intact. The pellet was lightly tapped and 2 mL of Bambanker serum-free cell freezing medium (Lymphotec Incorporated, Tokyo, Japan) was added to form a suspension. With each 2 mL suspension, 4-5 cryovials were produced and placed in an -80°C freezer for later use.

2.2: Reagents and Antibodies

For use in western blot experiments, the following items were purchased from commercial vendors: mouse monoclonal p53 primary detection antibodies (Santa Cruz Biotechnology Incorporated, Catalog Number: sc-126, Lot H1903S), rabbit monoclonal α -tubulin primary detection antibodies (Cell Signaling Technology Incorporated, Catalog Number: 2125S, Lot 11H10), anti-rabbit IgG secondary detection antibodies (Cell Signaling Technology Incorporated, Catalog Number: 7074), and anti-mouse IgG

secondary detection antibodies (Cell Signaling Technology Incorporated, Catalog Number: 7076).

2.3: RNA Extraction

RNA was extracted from 60 mm plates at 80% confluency using an RNeasy Mini Kit with RNeasy spin columns, QIAGEN[®] Shredder, and RNase-Free DNase Set according to protocol provided by the manufacturer (QIAGEN[®] Incorporated). The RNA was then stored at -80°C until it was needed. The purity of the RNA was confirmed by using the NanoDrop ND-1000 spectrophotometer with 1 µL of RNA sample (Thermo Fisher Scientific).

2.4: Reverse Transcription

Complementary DNA (cDNA) was produced using the High Capacity cDNA Reverse Transcription achieve kit (Applied Biosystems). To produce cDNA, 1 µg of RNA was reverse-transcribed with a total volume of 20µL of 2X RT Master Mix (10x reverse transcriptase buffer, 25x deoxyribonucleotide triphosphate mix, 10x RT random primer, MultiScribe[™] reverse transcriptase, RNase inhibitor, and nuclease-free water). A four-step reaction was conducted in a thermal cycler: 10 minutes at 25°C, 120 minutes at 37°C, 5 minutes at 85°C, and infinite minutes at 4°C. The generated cDNA was then stored at -20°C for later use.

2.5: Quantitative Real-Time Polymerase Chain Reaction Analysis (qRT-PCR)

qRT-PCR is a method utilized to measure mRNA expression in cells. Previously generated cDNA is needed for this assay, and is obtained from the Reverse Transcription assay, as described in chapter 2.4. Taqman® qRT-PCR was performed using primers to the two genes of interest (Tarsh and p53), and also the housekeeping gene glyceraldehyde-3-phosphate-dehydrogenase (GAPDH). GAPDH served as a positive homogenous control. Taqman® Gene Expression Assay primer Mm00618913_m1 for Tarsh (Applied Biosystems), primer Hs01034249_m1 for p53 (Applied Biosystems), and Taqman® 20x GAPDH primer probe dye: FAM-MGB (Applied Biosystems) were utilized.

The qRT-PCR reaction was carried out in triplicate on a 96-well optical reaction plate. Each well was comprised of 5 µL cDNA, 10 µL Taqman® 2x Universal PCR Master Mix (Applied Biosystems), 1 µL 20x primer, 4 µL distilled water, for a total volume of 20 µL/well. Afterward, the GAPDH primers were diluted to a 1:10 ratio. The plate was then sealed with a self-adhesive optical cover, and placed into the qRT-PCR machine.

The cDNA was then amplified using the 7500 HT Fast Real-Time PCR System (Applied Biosystems). The process involved the following steps: activation for two minutes at 50°C, then denaturation for 20 seconds at 95°C, followed by 40 cycles of melting for three seconds at 95°C, and finally annealing/extending for 30 seconds at 60°C, respectively. Using SDS 2.2 software, the average $\Delta\Delta CT$ values were calculated and relative quantification (ΔRQ) was measured. Finally, the difference in ΔRQ values between the targets and GAPDH was calculated.

2.6: Western Blot Assay

Cellular proteins from each cell line were extracted from cultured cells. These proteins were resolved in 12% denaturing polyacrylamide gels with 0.1% SDS. The proteins were resolved for 1 hour and 30 minutes at 125 V in 1x SDS-PAGE running buffer. Next, the proteins were transferred onto a polyvinylidene difluoride membrane (BioRad Laboratories) after it was briefly soaked 100% methanol. The transfer occurred in a 1x transfer buffer solution at 8 mA, and was run overnight.

After the transfer was completed, it was necessary to block the membrane. The membrane was gently rocked in a solution comprised of 2.5 g of dry milk dissolved in 50 mL of 1x Tris-Buffered Saline and Tween-20 (TBST) for 30 minutes. The membrane was then washed three times for 5 minute periods. Afterward, the primary antibody was diluted in a 5% TBST/milk or 1% bovine serum albumin (BSA) solution to generate a 1:1000 concentration. The membrane was gently rocked overnight at 4°C. Next, the membrane was washed three times for 5 minutes each in TTBS. Adding the antibody to a TBST/milk solution produced a 1:10,000 secondary dilution. The membrane was then gently rocked in this solution for 1 hour at room temperature. The membrane was washed for two 10-minute periods and one 30-minute period in TTBS.

Next, the membrane was prepared for film exposure by placing the membrane in a solution comprised of 500 μ L of enhancer solution and 500 μ L of peroxide buffer for five minutes (Western Lightning Chemiluminescence Plus System). The membrane was then wrapped in saran wrap, placed inside a cassette, and taken to a dark room. Blue Devil autoradiography film (Genesee Scientific) was placed onto the membrane and the cassette

was closed for a specific amount of time, depending on the primary antibody used. Finally, the film was placed into a Kodak photo-processing developer machine for exposure.

2.7: Cell Proliferation Assay

In preparation for this experiment, cultured cells were allowed to reach between 40-60% confluency on 10 cm plates. Cells were then washed twice with 5 mL PBS, and then detached from their culture plates using 1 mL of trypsin and placing the cells in a 37°C incubator for 15 minutes. These cells were seeded in triplicate in 24-well cell culture plates, and diluted to a density of 2×10^3 cells/mL in medium. The cells were then placed in a 37°C incubator for a 24-hour growth period.

Following the initial growth period, the first triplicate was washed twice with 1 mL of PBS. After aspiration of the PBS, 200 μ L of trypsin was pipetted into each well. The cells were then placed back into the incubator for 15 minutes to allow for cell detachment. After detachment, cells from each well were placed into separate eppendorf tubes. A 20 μ L volume from each eppendorf tube was then pipetted into a hemocytometer (Improved Neubauer Haemocytometer) chamber for cell counting.

The hemocytometer was then placed under a light microscope, and cells were found to reside in a nine-box grid. Counting of the cells was performed in each of the four corner grids (Figure 10). An average number of cells per well was obtained by dividing the total number of counted cells by four. This was repeated for all three samples for each cell derivative. These steps were repeated daily, for a total of six days. After the end of

the assay, the data was compiled in Excel and a proliferation curve was generated for each cell line. Tarsh transfected cells were compared to their respective controls to determine the effects of Tarsh on proliferation. Similarly, A549 p53 KD cells were compared to A549 WT cells to ascertain the effects of p53 on proliferation.

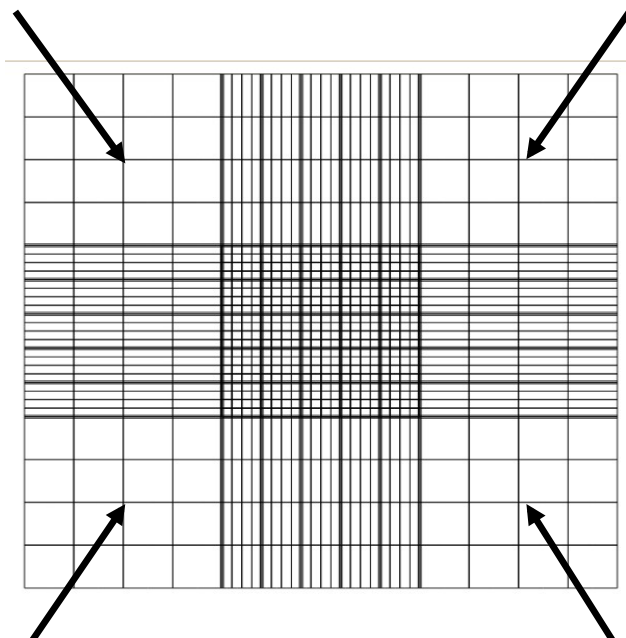


Figure 5: Hemocytometer Counting. Cell counting was performed in the four areas indicated by the arrows.

2.8: Cell Migration Assay

In preparation for this experiment, cultured cells were allowed to reach between 40-60% confluency on 10 cm plates. Cells were then washed twice with 5 mL PBS, and then detached from their culture plates using 1 mL of trypsin and placing the cells in a 37°C incubator for 15 minutes. These cells were seeded in triplicate in 24-well cell culture

plates, and diluted to a density of 2.5×10^5 cells/mL in medium. The cells were then placed in a 37°C incubator for a 24-hour growth period.

After the growth period, a sterile P200 pipette tip was utilized to create a scratch wound across each well (from top to bottom) in the 24-well plate. The scratch distance was measured at the time of the scratch (time = 0 hours). A ZEISS® Axiovert 200M microscope with AxioVision® digital image processing software was utilized to capture scratch distances in two different areas each scratch. Cells were then incubated for eight hours, resulting in the migration of cells and a reduction in the size of the scratch.

At the end of the incubation period (time = 8 hours), images were captured at the same two areas in each well. Each image at time = 8 hours was compared to its respective image at time = 0 hours. Tarsh transfected cell lines were compared to their respective controls to determine the effects of Tarsh on migration. Similarly, A549 p53 KD cells were compared to A549 WT cells to ascertain the effects of p53 on migration. To calculate the difference in migration, the following formula was used:

$$\text{Migration Rate} = \frac{(\text{Scratch distance at 0 hours}) - (\text{Scratch Distance at 8 hours})}{\text{Scratch Distance at 0 hours}} * 100\%$$

2.9: Statistical Analysis

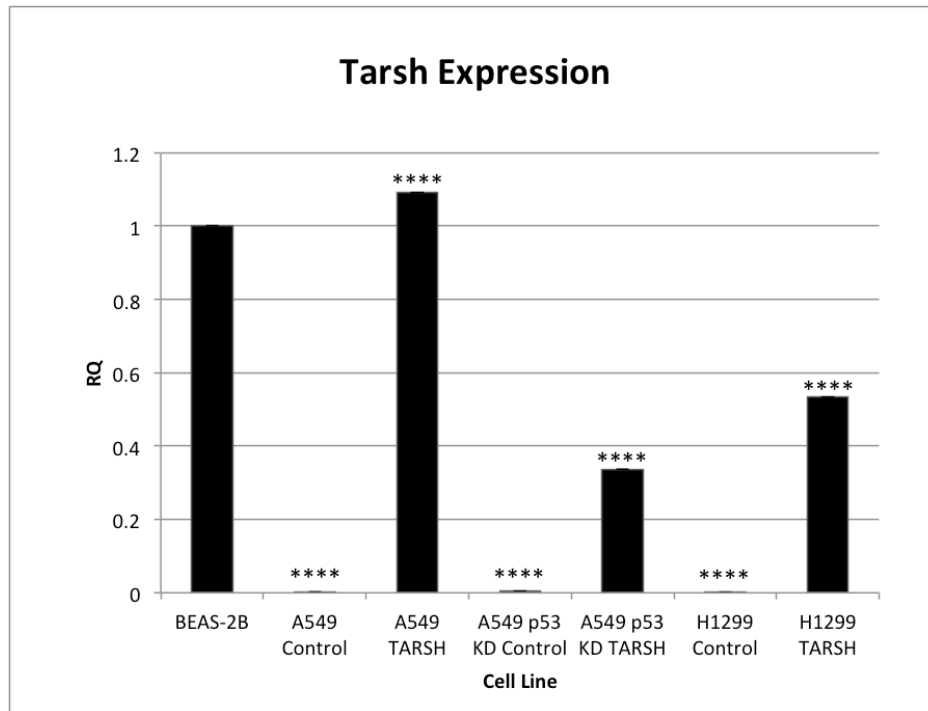
Comparisons between two groups were analyzed by using an unpaired *t*-test analysis with Excel and GraphPad software. A p-value < 0.05 was considered to be statistically significant.

Results

3.1: Tarsh Expression Confirmation with qRT-PCR Analysis

To investigate the biological role of Tarsh in A549 WT, A549 p53 KD, and H1299 cell carcinomas, the mRNA expression of Tarsh was examined in Tarsh transfected cell lines. For all of the cell types, BEAS-2B cells (normal epithelial lung cells) were used as a baseline for comparison. This information was needed before subsequent experiments could be performed to determine the effects of Tarsh on survival, proliferation, and migration.

In all of the lung cancer cell lines, all control cells were found to have a negligible expression of Tarsh. A549 WT Tarsh transfected cells were found to have 9.2% greater Tarsh expression, when compared to BEAS-2B cells. A549 p53 KD Tarsh transfected cells displayed a 66.3% reduction in Tarsh expression, when compared to BEAS-2B cells. Tarsh expression of H1299 Tarsh transfected cells was reduced by 56.7%, when compared to BEAS-2B cells. All of these differences were observed to be significant (Figure 6).



* $p < 0.05$, **** $p < 0.0001$

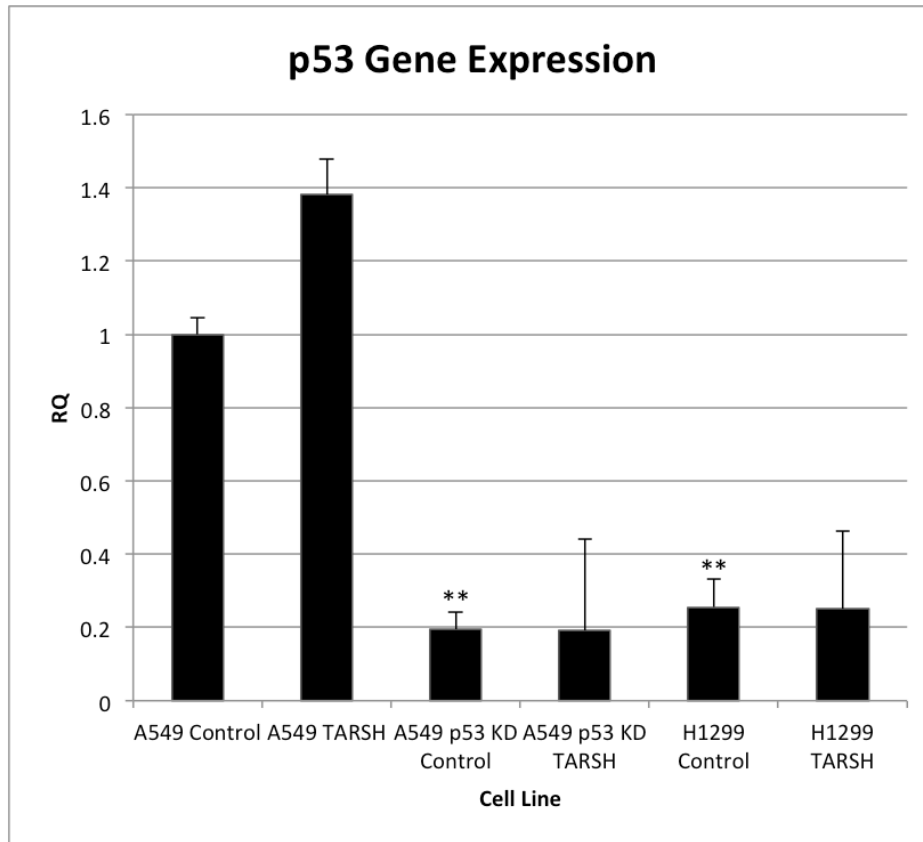
Figure 6: Tarsh Expression. RNA was extracted from near-confluent cultures of BEAS-2B, A549, and H1299 cells and reverse transcribed. Afterward, qRT-PCR was performed as previously described in Materials and Methods. Tarsh expression was standardized to the GAPDH, the homogenous control. The PCR was performed in triplicate and relative means \pm SEM are shown. A statistically significant decrease in Tarsh expression was found in A549 WT control cells, A549 p53 KD control cells, and H1299 control cells. A549 WT Tarsh transfected cells, A549 p53 KD Tarsh transfected cells, and H1299 Tarsh transfected cells displayed Tarsh expression within physiological ranges, thus confirming that any future experiments with these cell lines will be physiologically relevant.

3.2: p53 Downregulation Confirmation with qRT-PCR Analysis

To investigate the biological role of p53 in A549 WT, A549 p53 KD, and H1299 cell carcinomas, the mRNA expression of p53 was examined in these lung cancer cell lines. For all of the cell types, the A549 WT control cells were used as a baseline for comparison. This information was needed before subsequent experiments could be performed to determine the effects of p53 on survival, proliferation, and migration.

A549 WT Tarsh transfected cells were found to have 38.1% higher levels of p53 expression compared to the A549 WT control cells. However, this was not found to be statistically significant and was considered to be similar to the baseline. Both A549 p53 KD control cells, and A549 p53 KD Tarsh transfected cells showed a significant decrease in p53 expression, with an 81.6% reduction (Figure 7).

Similarly, both H1299 control cells and H1299 Tarsh transfected cells displayed a significant decrease in p53 expression, with a 75% reduction (Figure 7). Although this PCR experiment suggests that some p53 expression is still present in H1299 cells, this is not true of H1299 cells. As confirmed by previous findings⁽¹⁵⁾, and by the western blot to be discussed in the next section, these cells do not produce any functional p53 protein. This discrepancy can be explained by the fact that the p53 probe used in this experiment is detecting the partially deleted p53 gene in these cells.



** p < 0.01

Figure 7: p53 Gene Expression. RNA was extracted from near-confluent cultures of A549 and H1299 cells and reverse transcribed. Afterward, qRT-PCR was performed as previously described in Materials and Methods. The p53 expression was standardized to the GAPDH, the homogenous control. The PCR was performed in triplicate and relative means \pm SEM are shown. A statistically significant decrease in p53 expression was found in A549 p53 KD cell lines and H1299 cell lines, when compared to A549 WT control cells.

3.3: p53 Protein Expression Confirmation with Western Blot

To validate the previous results of the qRT-PCR in regards to p53 (Figure 2), it was necessary to perform a western blot analysis. A549 WT, A549 p53 KD, and H1299 cells were lysed, and gel electrophoresis was performed. The proteins were then transferred onto a membrane, which were detected with specific antibodies. This protocol was previously described in Materials and Methods. In this experiment, α -tubulin was used as the control.

The results of this experiment confirm the previous results of the qRT-PCR in regards to p53. It is clear that p53 protein expression levels in A549 WT cells are similar to that of tubulin. In addition, p53 protein expression is significantly downregulated in A549 p53 KD cell lines. In regards to H1299 cell lines, the western blot shows that these cells are not producing p53 protein (Figure 8).

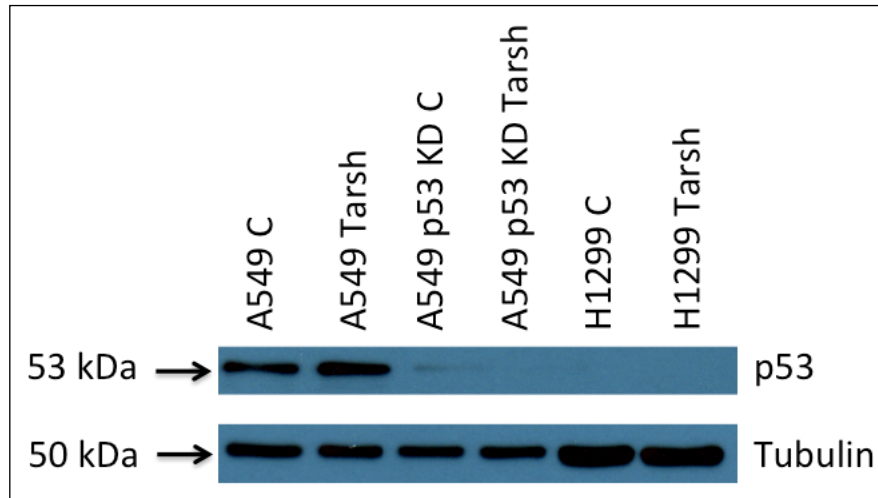
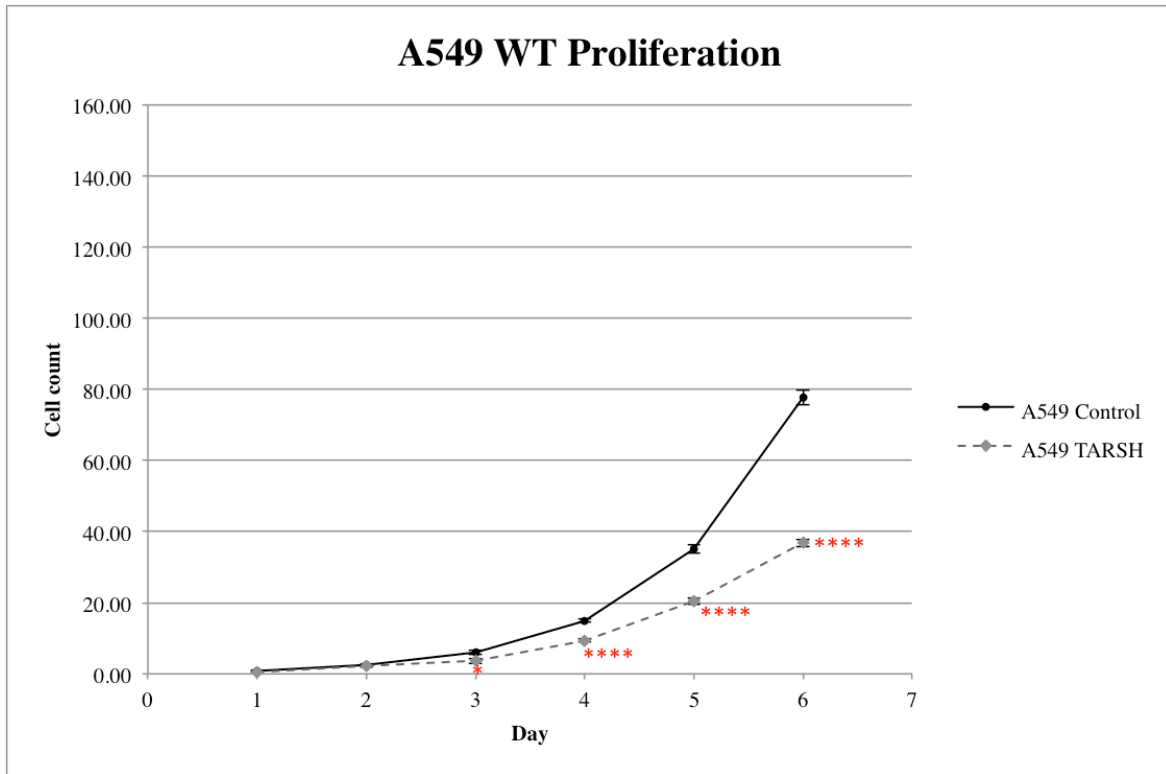


Figure 8: Western Blot Analyzing p53 Protein Expression. A549 WT, A549 p53 KD, and H1299 cells were lysed and gel electrophoresis was performed. The proteins were subsequently transferred to a membrane, and specific antibodies were utilized to determine the total molecule content of tubulin and p53. Tubulin was the control in this experiment. A549 WT cell lines had a comparable amount of p53 protein to tubulin. A549 p53 KD cell lines displayed a significant reduction in p53 protein production. H1299 cell lines did not produce p53 protein. Three trials were performed for this experiment.

3.4: Tarsh Overexpression Suppresses Proliferation in All Cell Lines

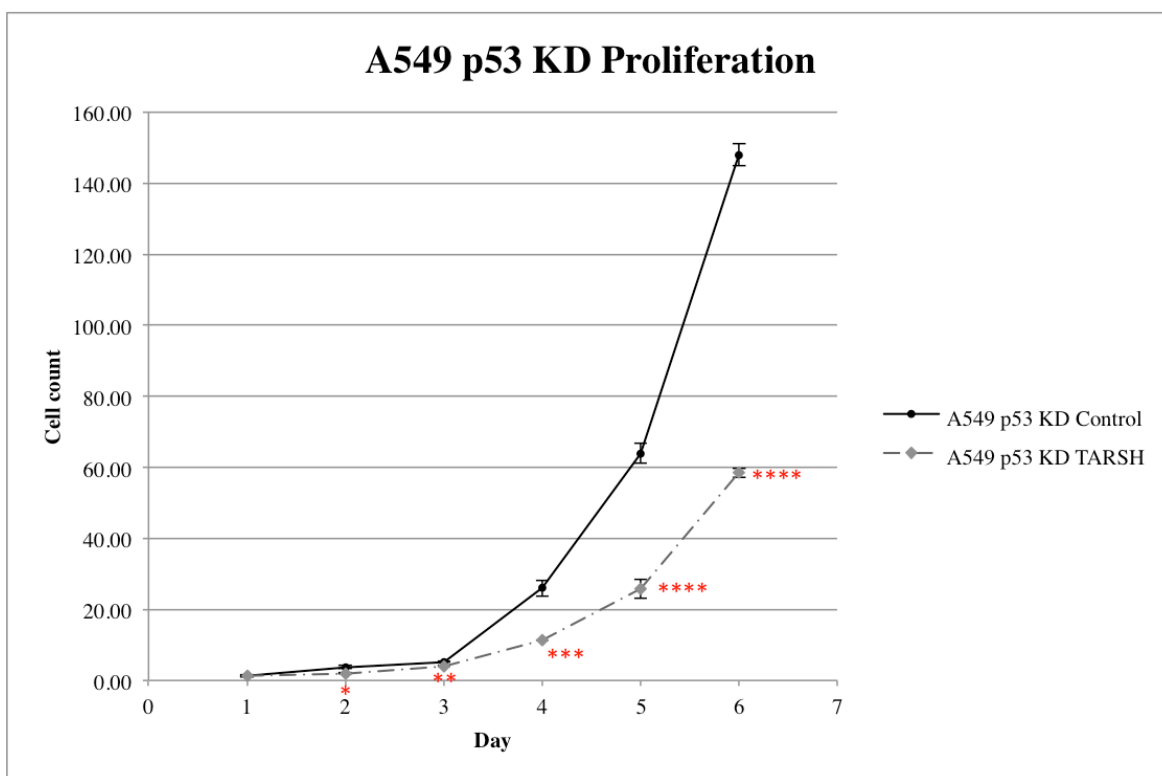
The proliferation and growth of cells in lung cancer contribute to the progression and metastasis of the disease. Therefore, it was important to observe the proliferation rates of all the cell lines involved in the study. Once the stability of the Tarsh transfected cell lines was confirmed by qRT-PCR (Figure 6), the cells were prepared for cell proliferation assays to measure their growth rates. In these assays, each cell line's respective control vector served as a basis for comparison. Each cell line was diluted to a density of 5×10^3 cells/mL in its respective selection medium conditions. The cells were then plated, in triplicate, onto 24-well plates (though only 18 wells were needed). A 24-hour latency period was allowed for initial growth to occur. For the following six days, cells in three out of the 18 wells were trypsinized and counted. The triplicated results were then averaged.

As shown in Figure 9, A549 WT Tarsh transfected cells exhibited an average reduction of 38% in growth when compared to A549 WT control cells. Starting from day 3, a statistically significant difference was observed with a p-value < 0.05 . From days 4-6, the difference was extremely significant, with a p-value < 0.0001 . Similarly, the average proliferation of A549 p53 KD Tarsh transfected cells was reduced by about 40% when compared to A549 p53 KD control cells (Figure 10). This decrease was also found to be statistically significant starting from day 2. Finally, Figure 11 shows that Tarsh also suppresses proliferation rates in H1299 cell lines. H1299 Tarsh transfected cells exhibited an average reduction of about 33% in growth when compared to H1299 control cells. The difference in growth was considered to be statistically significant.



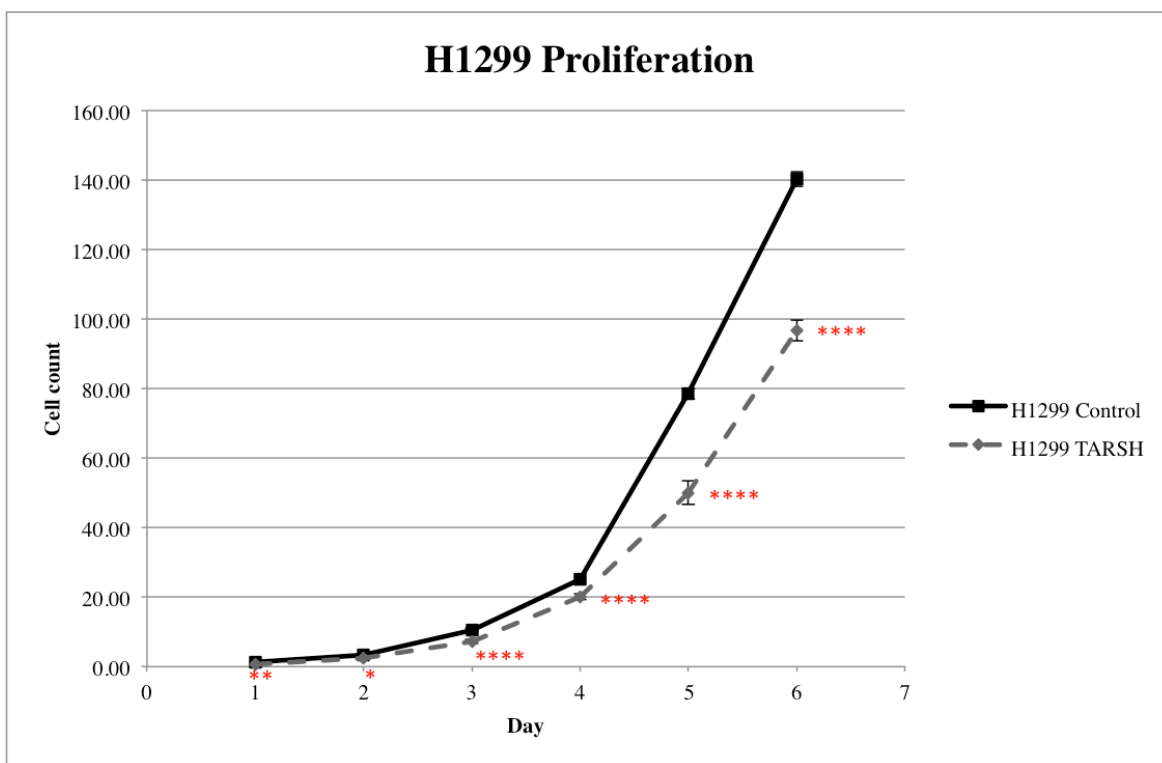
* p < 0.05, **** p < 0.0001

Figure 9: A549 WT Proliferation. A549 WT cells were diluted to a density of 2×10^3 cells/mL and were allowed a 24-hour growth period before counting began. In each trial, the cells were seeded in triplicate. An average number of cells were calculated each day for a total of six days. The mean cell counts and the \pm SEM are shown. Starting from day 3, a significant reduction in proliferation was observed in A549 WT Tarsh transfected cells when compared to A549 WT control cells. The number of trials ranged from six to seven for each cell line.



* p < 0.05, ** p < 0.01, *** p < 0.001, **** p < 0.0001

Figure 10: A549 p53 KD Proliferation. A549 p53 KD cells were diluted to a density of 2×10^3 cells/mL and were allowed a 24-hour growth period before counting began. In each trial, the cells were seeded in triplicate. An average number of cells were calculated each day for a total of six days. The mean cell counts and the \pm SEM are shown. Starting from day 2, a significant reduction in proliferation was observed in A549 p53 KD Tarsh transfected cells when compared to A549 p53 KD control cells. The number of trials ranged from three to five for each cell line.



* p < 0.05, ** p < 0.01, **** p < 0.0001

Figure 11: H1299 Proliferation. H1299 cells were diluted to a density of 2×10^3 cells/mL and were allowed a 24-hour growth period before counting began. In each trial, the cells were seeded in triplicate. An average number of cells were calculated each day for a total of six days. The mean cell counts and the \pm SEM are shown. A significant reduction in proliferation was observed in H1299 Tarsh transfected cells when compared to H1299 control cells. Six trials were performed for each cell line.

3.5: p53 Downregulation Increases Proliferation in All Cell Lines

In addition to observing the effects of Tarsh on cell growth, it was also important to determine the effects of downregulating p53 on the proliferation rates of all the cell lines involved in the study. A direct comparison between A549 WT and A549 p53 KD cells cannot be made due to differing selection medium conditions between the two. However, it can be inferred from the results that reducing p53 expression via knockdown in A549 cells increases proliferation, as A549 WT cells (Figure 9) generally had a higher cell count than A549 p53 KD cells (Figure 10). Similarly, although a direct comparison between A549 WT cells and H1299 cells cannot be made due to the fact that they are different cell lines, A549 WT cells (Figure 9) generally had a higher cell count than H1299 cells (Figure 11). This implies that the lack of p53 in H1299 cells caused an increase in the number of cells.

3.6: Tarsh Suppresses A549 Migration, H1299 Migration Unaffected

In vitro motility studies can give an indication of how readily a cancer metastasizes and spreads to distant areas of the body. Therefore, it was also important to observe the effects of Tarsh overexpression on cellular migration, in addition to proliferation. To observe the motility of A549 WT and A549 p53 KD cell lines, migration assay were performed. Each cell line was seeded across six wells, with each well yielding quadruplicate measurements. Each cell line was diluted to a density of 2.5×10^5 cells/mL, and the cells were allowed to grow to 100% confluency. A scratch was made on each well, and the cells were then incubated for eight hours. At the end of the incubation period, the cellular migration was calculated using AxioVision[®] software (Figure 12).

A549 WT Tarsh transfected cells displayed a statistically significant reduction in migration compared to A549 WT control cells. The difference in migration was 18.5%, with a p-value < 0.01 . Similarly, A549 p53 KD Tarsh transfected cells displayed a statistically significant reduction in migration compared to A549 p53 KD control cells. The migration was reduced by 18.2%, and the p-value was less than 0.05 (Figure 13).

However, Tarsh overexpression did not have any effect on H1299 cell migration. With a difference of only 1.4%, there was no statistically significant reduction when comparing H1299 Tarsh transfected cells to H1299 control cells (Figure 14).

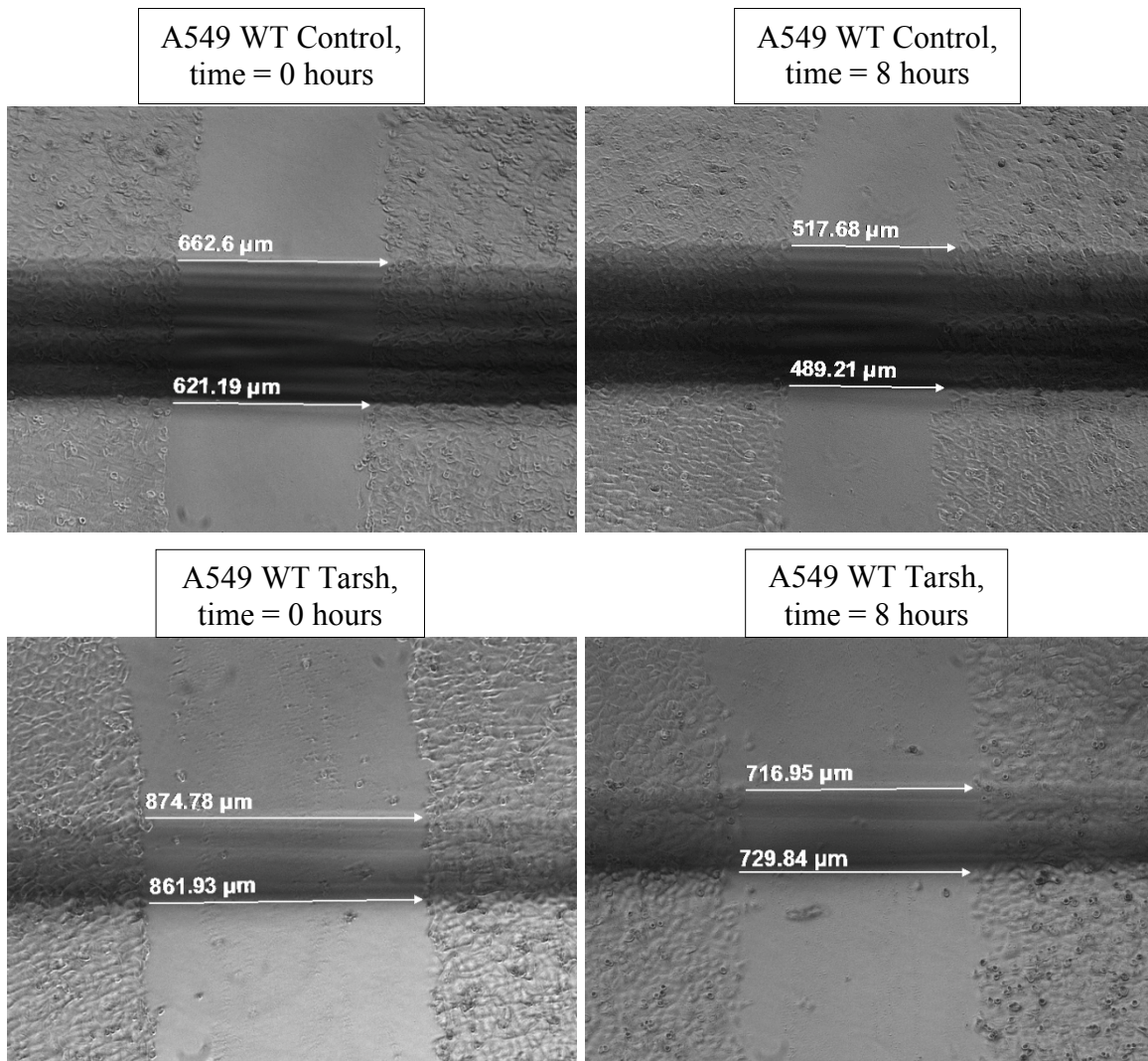
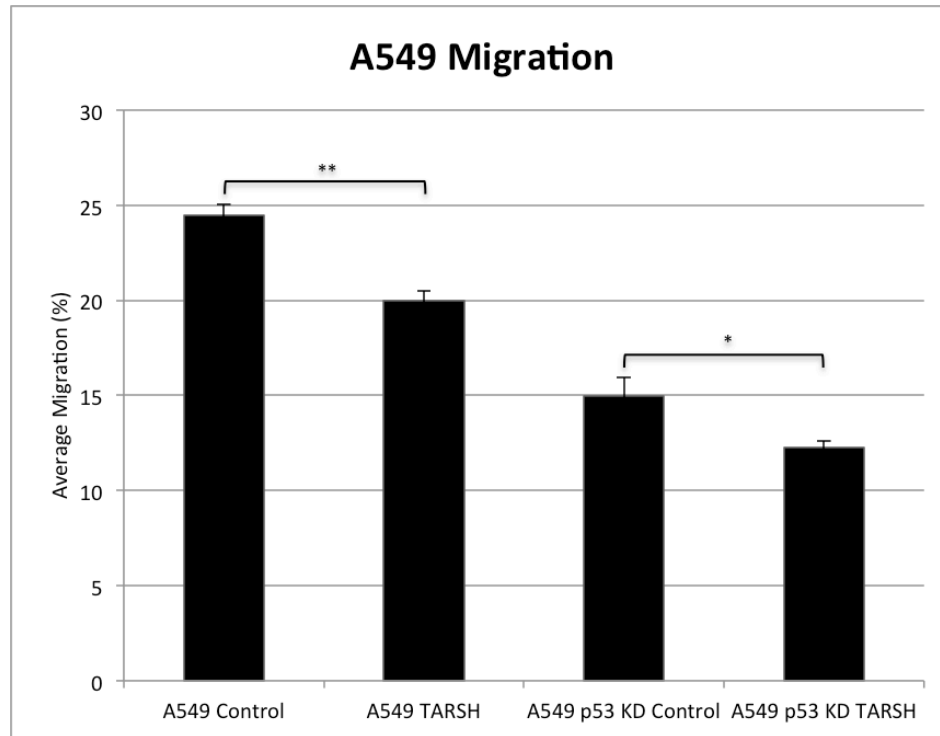


Figure 12: Cell Migration Assay. A549 WT and A549 p53 KD cells were plated at a density of 2.5×10^5 cells/mL, and were allowed to reach 100% confluency in their respective selection medium conditions. The migration assay was performed at time = 0 hours. After an 8-hour incubation period, the migration distances were measured with a ZEISS® Axiovert 200M microscope and AxioVision® digital imaging software. Representative images of A549 WT cells are shown at 0 and 8 hours.



* $p < 0.05$, ** $p < 0.01$

Figure 13: Role of Tarsh in A549 Migration. A549 cells were diluted to a density of 2.5×10^5 cells/mL and cultured to confluency. In each trial, the cells were seeded in quadruplicate. After reaching confluency, a migration assay was performed. A cell retardation ratio was then calculated based on the migration distance after 8 hours. The ratios were then averaged and the \pm SEM for each cell line was calculated. A549 WT Tarsh transfected cells displayed a significant reduction in migration compared to A549 WT control cells. Similarly, A549 p53 KD Tarsh transfected cells displayed a significant reduction in migration compared to A549 p53 KD control cells. The number of trials ranged from five to six for each cell line.

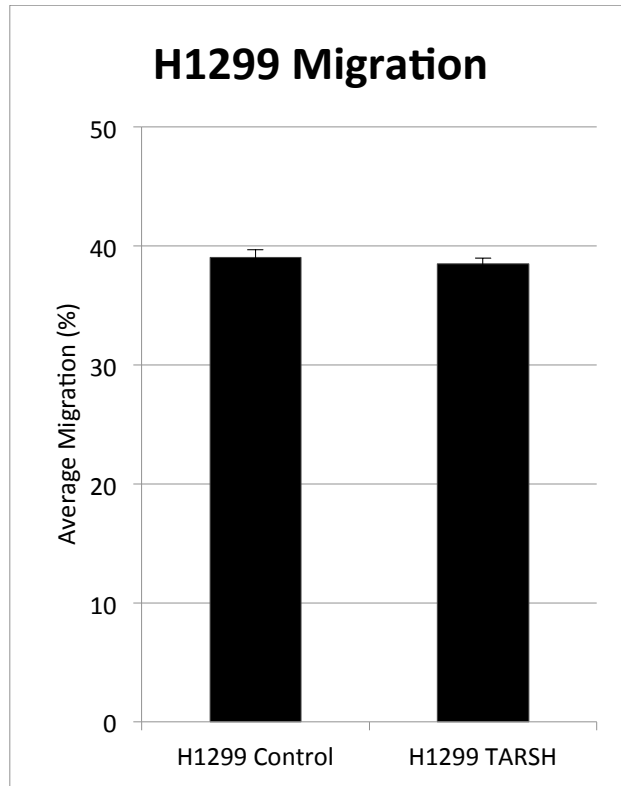


Figure 14: H1299 Migration. H1299 cells were diluted to a density of 2.5×10^5 cells/mL and cultured to confluency. In each trial, the cells were seeded in quadruplicate. After reaching confluency, a migration assay was performed. A cell retardation ratio was then calculated based on the migration distance after 8 hours. The ratios were then averaged and the \pm SEM for each cell line was calculated. No significant difference in migration was observed between the two cell lines. The number of trials ranged from four to five for each cell line.

3.7: Role of p53 in Migration is Unclear

In addition to Tarsh, it was also necessary to observe the effects of p53 downregulation on cellular motility. A direct comparison between A549 WT and A549 p53 KD cells cannot be made due to differing selection medium conditions between the two. However, it can be inferred from the results that reducing p53 expression via knockdown in A549 cells decreases the migration rate, as A549 p53 KD cells generally had a reduced migration distance when compared to A549 WT cells (Figure 13).

However, the opposite was observed when comparing A549 WT cells to H1299 cells. Although a direct comparison between A549 WT cells and H1299 cells cannot be made due to the fact that they are different cell lines, H1299 cells (Figure 14) generally had a higher migration distance when compared to A549 WT cells (Figure 13). In this case, the results imply that reducing p53 expression in cells increases the migration rate.

Discussion

4.1: Aims of the Current Study

The conclusions made by previous studies have shown that Tarsh expression is often downregulated in various cancer cell lines, and that re-expression of Tarsh significantly reduces cell proliferation, migration, and survival^(13,24,28). These results suggest that the loss of Tarsh expression may play a vital role in the pathogenesis and progression of various types of cancers. In addition, a previous paper concluded that Tarsh is dependent upon p53, suggesting that without it, Tarsh may lose its effectiveness⁽¹²⁾. However, only a very limited number of studies have been published, and further investigation is needed. As a result, the combined effects of Tarsh and p53 on tumor development are yet to be fully determined.

4.2 The Lung Cancer Cell Carcinoma (LCCC) Model System

In order to effectively study the effects of Tarsh and p53 in LCCC, an *in vitro* approach was utilized. Before any experiments were performed, lung cancer cell lines

were prepared and maintained in culture. The first cell line was the A549 cell line. These cells were obtained from an explanted tumor of a 58-year-old Caucasian male. For this study, the A549 cell line was split, and one group was transfected with Tarsh. Each resulting group was then split again, and p53 expression was knocked down in each group. This procedure resulted in four cell derivatives: A549 WT control, A549 WT Tarsh transfected, A549 p53 KD control, and A549 p53 KD Tarsh transfected cells. The H1299 cell line was the second cell line, which was isolated from a lymph node metastasis in a 43-year-old Caucasian male. These cells were split, and one group was transfected with Tarsh, resulting in two derivatives: H1299 Control and H1299 Tarsh transfected cells.

First, it was necessary to determine the mRNA expression levels of Tarsh in these cells, due to the fact that half of the cell derivatives were previously transfected with Tarsh. Therefore, qRT-PCR analysis was performed in the aforementioned cell lines. The results of the analysis showed that each Tarsh transfected cell line had significantly higher Tarsh mRNA expression when compared to its respective control (Figure 6). This data provided some of the foundation of the current study that was needed before any biological assays could be performed.

It was also essential to determine the expression levels of p53, as its expression was knocked down in half of the A549 cell derivatives, and is non-existent in H1299 cells. For this signaling molecule, qRT-PCR and western blot analyses were performed. In these assays, the p53 expression in A549 WT control cells served as the baseline measurement. The results of both assays led to the conclusion that p53 expression was highly downregulated in both A549 p53 KD control and A549 p53 KD Tarsh transfected cells

(Figures 7 and 8). Similarly, it was shown that both H1299 control and H1299 Tarsh transfected cells also had significantly decreased p53 expression (Figures 7 and 8). However, in regards to H1299 cells, it must be stated that a discrepancy was observed between the two assays. The qRT-PCR assay suggests that some p53 is present in H1299 cells, while the western blot analysis suggests that the cells are not generating any p53 protein. This can be explained by the fact that the p53 probe used in this experiment is detecting the partially deleted p53 gene in these cells.

4.3: Role of p53 and Tarsh in Cell Proliferation

Previous research has indicated that the expression of Tarsh is downregulated in various cancer cells^(13,24,28). In addition, it is common for p53 functionality to be lost in cancer, resulting in severely reduced tumor suppression⁽⁸⁾. In turn, cells that express p53 and Tarsh inhibited cell proliferation^(13,27). Results from the current study indicate that a decrease in proliferation was observed due to increased Tarsh and increased p53 expression. However, these two genes seem to work independently.

Ectopic overexpression of Tarsh in A549 cell lines caused a significant reduction in proliferation, when compared to their respective controls (Figures 9 and 10). In A549 WT cells, an average reduction of 38.0% was observed. Similarly, in A549 p53 KD cells, proliferation was reduced by an average of 39.7%. H1299 cells behaved similarly to A549 cells; proliferation was reduced by an average of 33.4% in H1299 Tarsh transfected cells (Figure 11). These findings suggest that Tarsh has an inhibitory effect on proliferation,

independent of p53. This is due to the fact that regardless of the level of p53 expression, Tarsh was able to downregulate proliferation in all of the examined lung cancer cell lines.

Although the effects of p53 on cell proliferation could not be directly compared between the cell lines, either due to differing selection medium conditions or the fact that the compared groups contained different cell lines, it could be inferred from the data that p53 has an inhibitory effect on proliferation. It can be generalized that A549 p53 KD cells had a higher cell count than A549 WT cells due to the fact that its p53 expression was knocked down in A549 p53 KD cells. Similarly, it can also be generalized that H1299 cells also have a higher cell count because they do not express p53.

4.4: Role of p53 and Tarsh in Cell Migration

Previous findings suggest that Tarsh and p53 expression suppresses cell motility in cancer cells^(13,17). The results of the current study support the notion that Tarsh overexpression reduces motility, but only in A549 cells. However, Tarsh overexpression in H1299 cells did not affect migration. Additionally, a concrete conclusion cannot be made in terms of the effects of p53 on migration, due to varying results.

The overexpression of Tarsh in A549 cell lines caused a significant reduction in migration, when compared to their respective controls (Figure 13). In A549 WT cells, an average reduction of 18.5% was observed. Likewise, in A549 p53 KD cells, proliferation was reduced by an average of 18.2%. These findings suggest that Tarsh has an inhibitory effect on migration, independent of p53. This is due to the fact that regardless of the level of p53 expression, Tarsh was able to downregulate migration in A549 cells.

However, H1299 cell migration was not affected by ectopic Tarsh overexpression; only a 1.4% difference in migration was observed (Figure 14). These results could be explained by the fact that H1299 cells do not have functional p53⁽¹⁵⁾, and are therefore different from A549 cells. Due to the complete lack of p53 in H1299 cells, they may lack a p53-dependent pathway in which migration is dependent on in A549 cells. It could be possible that H1299 cells have circumvented this pathway, or may have even developed a novel pathway that affects migration. Although p53 expression was highly downregulated in A549 p53 KD cells, this was artificially created. In reality, A549 cells do express endogenous p53. Therefore, it is likely that a p53-dependent pathway still exists in A549 p53 KD cells.

Although the effects of p53 on cell migration could not be directly compared between the cell lines, either due to differing selection medium conditions or the fact that the compared groups contained different cell lines, it could be inferred from the data that p53 has opposing effects in A549 cells and H1299 cells. It can be generalized that A549 p53 KD cells had a reduced migration rate, when compared to A549 WT cells, due to the fact that its p53 expression was knocked down in A549 p53 KD cells. These observations do not support previous findings. However, it can also be generalized that H1299 cells, which lack p53, was observed to have the highest migration rate. These results do support previous findings. The unexpected results of the A549 p53 KD migration assays could possibly be explained by the use of a differing selection medium. These cells were grown in a puromycin selection medium, whereas A549 WT and H1299 cells were grown in a

neomycin and puromycin selection medium. It is possible that the differing conditions could have impacted the results.

4.5: Conclusions

In this study, it was shown that ectopic overexpression of Tarsh in lung cancer cell lines decreased cell proliferation and migration, independent of p53. Additionally, decreased p53 expression levels coincided with an increase in cell proliferation. However, the role of p53 in LCCC migration remains unclear. At this point, a more detailed understanding of the pathway by which Tarsh and p53 interact is required to make more concrete conclusions. Regardless of this fact, this field of research seems promising in that it may lead to the development of novel treatments that can suppress tumor malignancy.

4.6: Future Studies

Given that p53 is mutated in many types of cancer⁽⁸⁾, supplemental experiments focusing on cell lines with mutated p53 could be utilized. KNS-62, an epithelial cell line derived from a brain metastasis of a primary lung tumor⁽²²⁾, has been prepared for future experiments. Stable Tarsh transfects were produced using the GeneCopoeia® HIV-based lentiviral expression vector system. Tarsh expression was confirmed via qRT-PCR. The resulting cell derivatives, KNS-62 control cells and KNS-62 Tarsh transfected cells, were frozen, made into stock, and stored at -80°C. These cells are ready to be utilized in proliferation and migration assays.

In addition, it is necessary to reexamine cell migration in A549 p53 KD cell lines. The results obtained from this study do not follow the trend that was observed in previous studies, as well as H1299 cells. As explained in the discussion section, a possible reason for this outcome could be due to the selection medium used for A549 p53 KD cells. Repeating the migration experiments with the same selection medium conditions as A549 WT and H1299 cell lines may lead to a more reliable conclusion.

Literature Cited

Literature Cited

1. **Abbas T, Dutta A.** p21 in Cancer: Intricate Networks and Multiple Activities. *Nat Rev Cancer.* 2009; 9(6): 400-414.
2. **Bai L, and Wei-Guo Zhu.** p53: Structure, Function and Therapeutic Applications. *Journal of Cancer Molecules.* 2006; 2(4): 141-153.
3. **Chen LL, Blumm N, Christakis NA, Barabási, AL, Deisboeck TS.** Cancer Metastasis Networks and the Prediction of Progression Patterns. *British Journal of Cancer.* 2010; 101: 749-758.
4. **Chène, P.** The Role of Tetramerization in p53 Function. *Oncogene.* 2001; 20(21): 2611-2617.
5. **Division of Cancer Prevention and Control.** Lung Cancer. *Centers for Disease Control and Prevention.* 2013.
6. **Harms KL, Chen X.** The C Terminus of p53 Family Proteins is a Cell Fate Determinant. *Mol. Cell. Biol.* 2005; 25(5): 2014-2030.
7. **Herbst RS, Bajorin DF, Bleiberg H, Blum D, Hao D, Johnson BE, Ozols RF, Demetri GD, Ganz PA, Kris, MG, Levin B, Markman M, Raghavan D,**

- Reaman GH, Sawaya R, Schuchter LM, Sweetenham JW, Vahdat LT, Vokes EE, Winn RJ, Mayer RJ.** Clinical Cancer Advances 2005: Major Research Advances in Cancer Treatment, Prevention, and Screening – A Report from the American Society of Clinical Oncology. *American Society of Clinical Oncology*. 2006; 24: 190-205.
8. **Hollstein M, Sidransky D, Vogelstein B, Harris CC.** p53 Mutations in Human Cancers. *Science*. 1991; 253(5015): 49-53.
9. **Howlander N, Noone AM, Krapcho M, Neyman N, Aminou R, Altekruse SF, Kosary CL, Ruhl J, Tatalovich Z, Cho H, Mariotto A, Eisner MP, Lewis DR, Chen HS, Feuer EJ, Cronin KA.** SEER Cancer Statistics Review, 1975-2009 (Vintage 2009 Populations). *National Cancer Institute*. 2012.
10. **Isobe M, Emanuel BS, Givol D, Oren M, Croce CM.** Localization of Gene for Human p53 Tumour Antigen to Band 17p13. *Nature*. 1986; 320(6057): 84-85.
11. **Kim MM, Califano JA.** Molecular Pathology of Head and Neck Cancer. *International Journal of Cancer*. 2004; 112: 545-553.
12. **Larsen S, Yokochi T, Isogai E, Nakamura Y, Ozaki T, Nakagawara A.** LMO3 interacts with p53 and inhibits its transcriptional activity. *Biochem. Biophys. Res. Commun*. 2010; 392(3): 252-257.

13. **Latini FRM, Hemerly JP, Freitas, Beatriz CG, Oler G, Riggins GJ, Cerutti, J.** ABI3 Ectopic Expression Reduces in vitro and in vivo Cell Growth Properties While Inducing Senescence. *M BMC Cancer*. 2011; 11: 11.
14. **Levine, A. J. & Oren, M.** The First 30 Years of p53: Growing Ever More Complex. *Nature Reviews Cancer*. 2009; 9: 749-758.
15. **Lin DL, Chang C.** p53 is a Mediator for Radiation-repressed Human TR2 Orphan Receptor Expression in MCF-7 Cells, a New Pathway from Tumor Suppressor to Member of the Steroid Receptor Superfamily. *J. Biol. Chem.* 1996; 271 (25): 14649-14652.
16. **Matlashewski G, Lamb P, Pim D, Peacock J, Crawford L, Benchimol S.** Isolation and Characterization of a Human p53 cDNA Clone: Expression of the Human p53 Gene. *EMBO J.* 3(13): 1984; 3257-3262.
17. **Muller PAJ, Vousden KH, Norman JC.** p53 and Its Mutants in Tumor Cell Migration and Invasion. *J Cell Biol.* 192(2): 2011; 209-218.
18. **National Cancer Institute.** Cancer Topics. *National Institutes of Health*. 2013.
19. **Pichandi S, Pasupathi P, Rao YY, Farook J, Ponnusha BS, Athimoolam A, Subramaniyam S.** The Effect of Smoking on Cancer-A review. *International Journal of Biological and Medical Research*. 2011; 2: 593-602.

20. **Pöschl G, Seitz, HK.** Alcohol and Cancer. *Alcohol and Alcoholism*. 2004; 39: 155-165.
21. **Read AP, Strachan T.** Human Molecular Genetics 2. *New York: Wiley*. 1999; Chapter 18: Cancer Genetics.
22. **Takaki T.** An Epithelial Cell Line (KNS-62) Derived From a Brain Metastasis of Bronchial Squamous Cell Carcinoma. *Journal of Cancer Research and Clinical Oncology*. 1980; 96(1): 27-33.
23. **Terauchi K, Shimada J, Uekawa N, Yaoi T, Maruyama M, Fushiki S.** Cancer-associated Loss of TARSH Gene Expression in Human Primary Lung Cancer. *Journal of Cancer Research and Clinical Oncology*. 2006; 132(1): 28-34.
24. **Thun, MJ; Hannan LM, Adams-Campbell LL et al.** Lung Cancer Occurrence in Never-Smokers: An Analysis of 13 Cohorts and 22 Cancer Registry Studies. *PLoS Medicine*. 2008; 5(9): e185.
25. **Uekawa, N, Terauchi K, Nishikimi A, Shimada J, Maruyama M.** Expression of TARSH Gene in MEFs Senescence and its Potential Implication in Human Lung Cancer. *Biochemical and Biophysical Research Communications*. 2005; 329(3): 1031-1038.
26. **Venot C, Maratrat M, Dureuil C, Conseiller E, Bracco L, Debussche L.** The Requirement for the p53 Proline-Rich Functional Domain for Mediation of

Apoptosis is Correlated with Specific PIG3 Gene Transactivation and with Transcriptional Repression. *EMBO J.* 1998; 17(16): 4668-4679.

27. **Ventura A, Kirsch D, McLaughlin M, Tuveson DA, Grimm J, Lintault L, Newman J, Reczek EE, Weissleder R, Jacks T.** Restoration of p53 Function Leads to Tumour Regression in vivo. *International Weekly Journal of Science.* 2013; 445: 661–665.
28. **Wakoh T, Uekawa N, Terauchi K, Sugimoto M, Ishigami A, Shimada J, Maruyama M.** Implication of p53-dependent cellular senescence related gene, TARSH in tumor suppression. *Biochemical and Biophysical Research Communications.* 2009; 380(4): 807-812.
29. **Winstanley MH, Pratt IS, Chapman K, Griffin HJ, Croager EJ, Olver IN, Sinclair C, Slevin TJ.** Alcohol and cancer: a position statement from Cancer Council Australia. *The Medical Journal of Australia.* 2011; 194: 479-482.
30. **Young C.** Solar ultraviolet radiation and skin cancer. *Occupational Medicine.* 2009; 59: 82-88.

VITA

Young Min Kim was born in Dover, NJ on February 6, 1985. He has lived in Charlotte, NC since the age of four, and more recently, in Richmond, VA. He graduated from Providence Senior High School in Charlotte, NC in 2003. He went on to receive a B.S. in Biology from the Virginia Tech in 2007. After completing his undergraduate study, he pursued a Master of Science in Physiology at the VCU School of Medicine. He will go on to continue his education within the VCU School of Dentistry starting in the fall of 2013.